Influence of Harmonic Current on the AC losses of a Tri-axial REBCO Cable for Hybrid Electric Aircraft

Zixuan Zhu, Yawei Wang, Sriharsha Venuturumilli, Jie Sheng, Min Zhang, Weijia Yuan

***Abstract*—High temperature superconducting (HTS) tri-axial CORC cable has been a potential candidate for the transmission line used in an all-electric aircraft because of its advantages such as compactness, high power density and reduced usage of HTS tapes. A tri-axial CORC HTS cable (10 MW, 3 kV/2 kA) is being developed in University of Bath in cooperating with Airbus. AC/DC converters, generators and motors will induce harmonic currents in the power system of a hybrid electrical aircraft. It may considerably affect the AC loss of the transmission cable, which is one of the key factors determining the efficiency of the cable. This paper studies the transport AC losses of this tri-axial CORC cable and the influence of harmonic current on the losses. A finite element method (FEM) model has been developed based on T-A formulation to analyze the dynamic electromagnetic behavior of this tri-axial CORC cable. Analyses are performed under rated load with & without harmonic currents. Results show that the transport AC loss has a significant non-uniform distribution among three phases even under a three-phase balanced load. A small harmonic current (less than 10 %) can considerably increase the AC loss of the tri-axial cable (up to 40 %).**

***Index Terms*— HTS tri-axial CORC cable, Harmonic current, Ac loss, T-A formulation, Hybrid electric aircraft**

I. Introduction

The aerospace sector is actively pursuing revolutionary design concepts towards electric aircraft to further reduce the environmental impact of air travel, as well as to enhance competitiveness in the face of an predicable long-term rise in fuel cost. The emission of an all-electric aircraft is still distant because of the low energy density of present battery technology. Hybrid electric propulsion, on the other hand, is considered as a more practical design, in which power generator is drove by turbines and the propulsion system consists of electrical HTS motors [1-6]. The power requirement for a passenger aircraft ranges from 5 MW to 50 MW. If a conventional copper cable is used to deliver the power, the conductors would be too heavy to be practical, and losses generated during the transportation are likely to cause significant decrease in the efficiency of the aircraft, and even to outweigh any benefits [5, 7, 8].

The HTS cable shows great potential to be used in an hybrid electric aircraft, since the current-carrying capacity of HTS is more than twenty times that of materials such as copper [9]. By far, several HTS cables, such as twisted cable, Robel cable, and conductor on round core (CORC) cable, have been developed for all kinds of HTS applications [9-12]. The tri-axial CORC cable, however, is considered to be the most promising candidate for hybrid aircraft due to its advantages such as compactness, high power density and low cryogenic cost. The 3-phase delta-connected coaxial schemes significantly reduce the usage of ReBCO tapes, because the sum of 3-phase current vectors is always zero, leading to a small external magnetic field, thus the shielding layer and return path are not necessary [13-16].

University of Bath is developing an all-superconducting power system for hybrid electric aircrafts cooperating with Airbus [6]. By far, a 10 MW, 3kV/2kA tri-axial CORC cable is developed. Since AC loss is a key factor to determine the efficiency of the HTS cable, a detailed analysis is needed. Studies on AC losses have been carried out on many applications of HTS cables, such as accelerator magnet and transmission lines [17-20]. Existing research shows that the AC loss of CORC cable mainly depends on the applied current, frequency, pitch length, and external magnetic field [9, 21-23]. In the power system of electrical aircraft, harmonic currents are easily and unavoidably induced inside AC/DC converters, generators and motors [24]. It may cause a significant influence on the total AC losses of the cable.

This paper studies the transport AC losses of a 10 MW, 3kV/2kA tri-axial CORC cable designed for hybrid electric aircraft and the influence of harmonic currents on the AC losses. Detailed specification of the cable is presented. A numerical model is built based on T-A formulation to study the dynamic electromagnetic behaviors of the tri-axial CORC cable. The influence of the harmonic currents on the AC loss is analyzed.

II. The HTS cable and analysis tool

A. Specification of the tri-axial CORC cable for aircraft

The cable is designed to deliver 10 MW/3 phases from generator to propulsion motors with a compact space structure. Three electrical phases are concentrically arranged to form the tri-axial structure, as shown in Fig. 1. The cable is rated at 3kV, 2kA$_{rms}$ with an operating frequency of 50Hz. The given operating temperature of the cable is 70K. Each phase consists of 28 ReBCO tapes winding spirally around a cylindrical stainless-steel former. Width and thickness of the tape are 4mm and 1mm respectively, and each tape has a critical current of 150A in self-field at 70K. Peak value of the rated

Manuscript receipt and acceptance dates will be inserted here. Acknowledgment of support is placed in this paragraph as well. *(Corresponding author: Weijia, Yuan, w.yuan@bath.ac.uk.)*

Zixuan Zhu, Yawei Wang, Sriharsha Venuturumilli, Jie Sheng, Min Zhang, Weijia Yuan are all with the Department of Electric and Electrical Engineering, University of Bath, UK, BA2 7AY, UK.

Color versions of one or more of the figures in this paper are available online at http://ieeexplore.ieee.org.

Digital Object Identifier will be inserted here upon acceptance

current is 100A. Liquid nitrogen is filled in the channel of both the inner and outer formers as refrigerant. The insulation layers between adjacent phases use Kapton as dielectric materials. The outermost layer uses copper as a shielding material and is connected to the ground to prevent the cable from damage caused by overrated voltages. More detailed specification is shown in Table I.

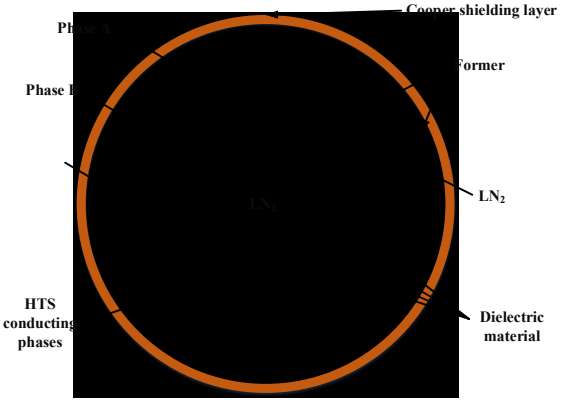

Fig. 1. The geometry of the HTS tri-axial CORC cable

TABLE I
SPECIFICATION OF THE HTS TRI-AXIAL CORC CABLE FOR AIRCRAFT

Parameters		Quantity
Cable	Phase	3
	Frequency	50
	Power	10 MW
	Voltage/Current	3 kV/2 $kA_{(rms)}$
ReBCO Tape	Width/Thickness	4mm/0.1mm
	Critical current, I_c @ 70K	150 A
	Operating current, peak, I_p	100 A
	Operating temperature	70 K
	Tapes per phase	28
Former, inner	Material	Stainless Steel
	Diameter/thickness	25mm/0.3mm
Former, outer	Material	Stainless Steel
	Diameter/thickness	99.2mm/2mm
Insulation	Material	Kapton
	Thickness	8 mm

B. The T-A model for tri-axial CORC cable

The HTS tri-axial CORC cable model was built using finite element method (FEM). A new set of formulation, which is called T-A formulation, was applied to develop the model. Main idea of the T-A formulation is to solve the problem of the high aspect ratio by approximating the superconducting tape to be a sheet, thus the thickness of the conductors can be ignored [25, 26]. The model space is divided into two parts, the superconducting region and the normal zone. Two state variables are used in this model, the current vector potential **T** and the magnetic vector potential **A**. T-formulation is used to build the superconducting region, while modeling of the normal zone uses A-formulation as its governing equation. The governing equation of this model is derived from Maxwell's equations [25]:

$$\begin{cases} \nabla \times \mathbf{T} = \mathbf{J} & \text{in } \Omega_{HTS} \\ \nabla \times \nabla \times \mathbf{A} = \mu \mathbf{J} & \text{in } \Omega_{normal} \end{cases} \quad (1)$$

For ReBCO conductor, the highly nonlinear relationship between current and the voltage can be expressed as:

$$\mathbf{E} = E_0 \left(\frac{\mathbf{J}}{J_c(\mathbf{B})}\right)^n \frac{\mathbf{J}}{|\mathbf{J}|} \quad (2)$$

where E_0=1 μV/cm, n=31, and J_c is the critical current density. The AC loss in superconducting layers is calculated by [27-29]:

$$W = \int_{\Omega_{HTS}} \mathbf{E} \cdot \mathbf{J} d\Omega \quad (3)$$

This model is built and solved using COMSOL Multiphysics, as shown in Fig. 2. Main advantage of the T-A formulation is that, by transforming a three-dimensional model into a two-dimensional one, it effectively reduces the mesh elements, thus fastening the computation time [25].

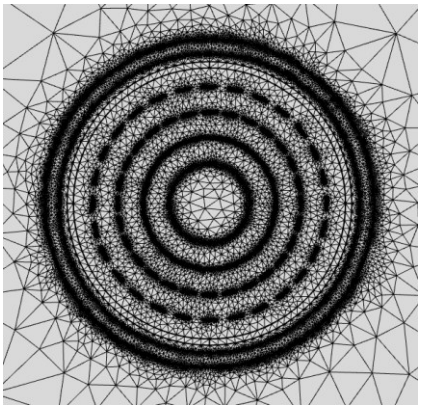

Fig. 2. The FEM model based on T-A formulation of a tri-axial CORC cable

III. ANALYSIS AND DISCUSSION

A. Balanced rated load without harmonic current

Fig. 3(a) shows the transport loss power of one cycle time under a balanced rated load. Although each phase has the same transport current, as shown in Fig. 3(b), the transport AC losses in three phases are still considerably imbalanced. Compared with the inner phase A, losses produced in the middle phase is doubled, while the outer phase C has the largest value of losses, three times more than that of the inner phase. As can be seen from Fig. 3(a) and Fig. 3(b), the peak value of the AC loss doesn't happen at the peak point of the transport current. This is because that the transport loss depends on both transport current and critical current, and the critical current is field dependent. In addition, the AC losses of HTS tapes on each phase are significantly affected by the other two phases through magnetic coupling process.

Fig. 4 shows the dependence of transport AC loss on the magnitude of the transport current under balanced load. Sharp increase of the AC losses can be seen from the operating current of 100A to 120A, which illustrates that the transport losses of the cable rise up with the operating current in a rapid way. As can be seen in Fig. 5, transport AC loss of each phase

shows a linear increase with the frequency of the transport current. It illustrates a frequency independent behavior of the AC loss energy per cycle (*J/cycle*) in the tri-axial CORC cable, which agreed with previous studies in other applications. Both the results in Fig. 4 and Fig. 5 show that the transport AC loss always presents a significant non-uniform distribution among three phases under different transport currents.

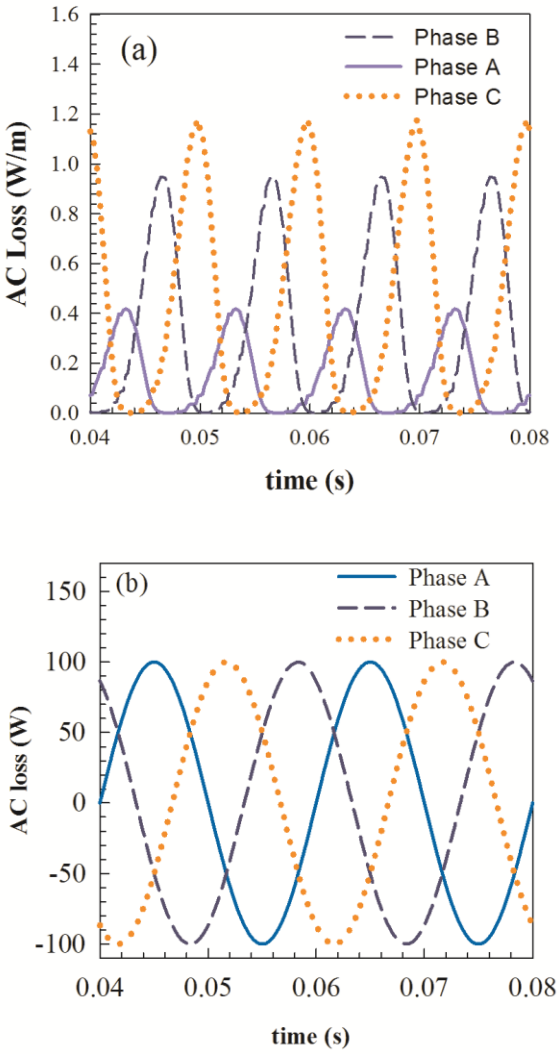

Fig. 3. Transport AC loss varying with time under rated load (100A, 50Hz)

B. Rated load with harmonic current

For comparison, harmonic currents have been applied to the model of the tri-axial cable to study the influence of the harmonics on AC losses of the cable. Fig. 6 shows the transport AC loss power under rated load with a harmonic current of 10A/200Hz on each phase. Compared with the results in Fig. 3(a), trend of the curve of the AC loss power is remarkably changed by the harmonic current. Three power peaks are induced during one cycle time as shown in Fig. 6.

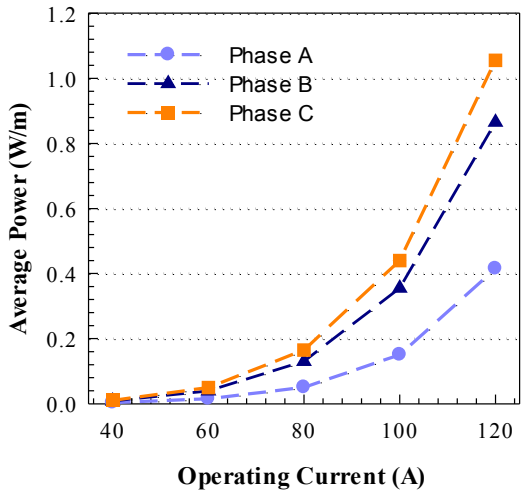

Fig. 4. Transport AC loss vs operating current

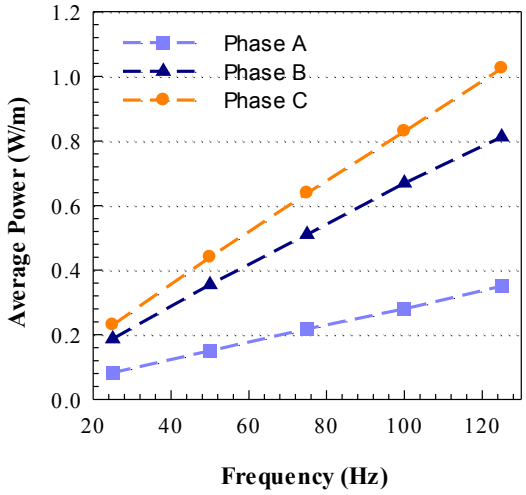

Fig. 5. Transport AC loss vs frequency

The maximum peak values of the AC loss power in each phase are all doubled after applying the harmonic currents to the cable. Fig. 9 shows the distribution of the normal magnetic field and the normalized current density at three peak points of AC loss power in Phase C. The background field of each phase is determined by the other two phases. The magnitude of the AC loss power depends not only on the applied current in one phase but also on the current in the other two phases. The comprehensive electromagnetic coupling leads to the AC loss power curve in Fig. 6.

In Fig. 7, the transport AC losses of the tri-axial cable are plotted against the harmonic current. Compared with Fig. 4, losses in phase A increase unexpectedly by around 53.3%, from 0.15W/m to 0.23W/m. Transport AC losses in phase C, on the other hand, only increase by 45.5%, from 0.44W/m to 0.64W/m. To further analyze the influence of the harmonic current on AC losses of the cable, a harmonic current of 10A was added to each phase. The increasing rate of transport AC losses against different operating frequencies are calculated and plotted in Fig. 8. Results show an increasing trend similar to Fig. 7, which is that, compared with other two phases, the inner phase A is most affected by the harmonic current. The

increasing rate of phase A considerably raises to about 45% while the increasing rates of phase B and C reach a peak value of 35%. Conclusion can then be obtained that when the same harmonic current has been applied simultaneously to each phase, the harmonic current has a minimal impact in the most outer phase and affects the inner phase the most. In addition, as shown in Fig. 8, a considerably sharp increase of losses in three phases occurs from frequency of 100Hz to 500Hz. The rate of increase then starts to slow down, finally enter a steady stage. This indicates that to minimize the transport AC losses, one should eliminate harmonic currents with high frequencies and high amplitudes.

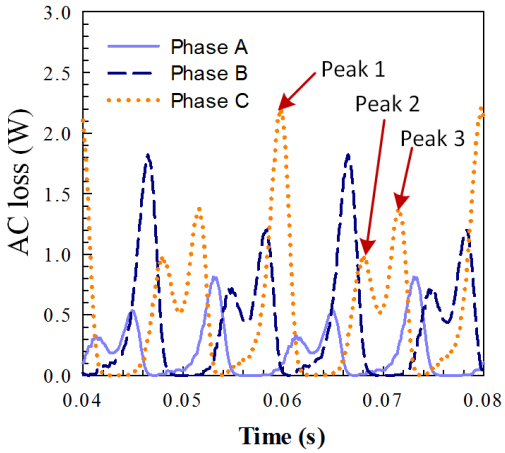

Fig. 6. Transport AC losses under balanced rated load with a harmonic current (10A, 200Hz)

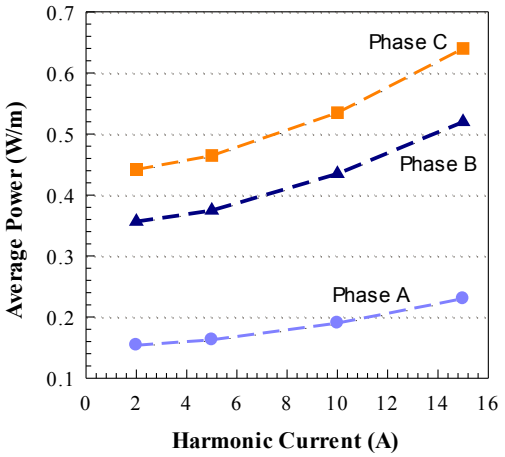

Fig. 7. Transport AC losses vs harmonic current with a fixed frequency of 200Hz

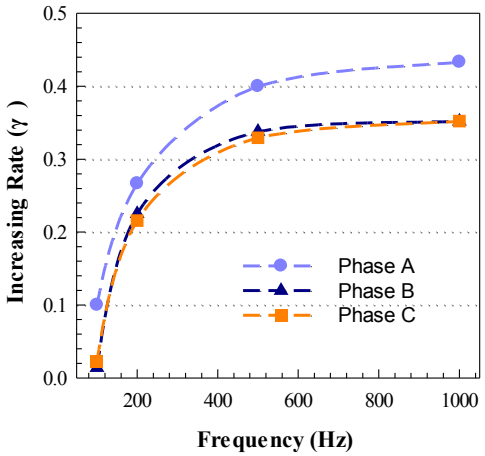

Fig. 8. Transport AC losses vs frequency with a fixed harmonic current of 10A

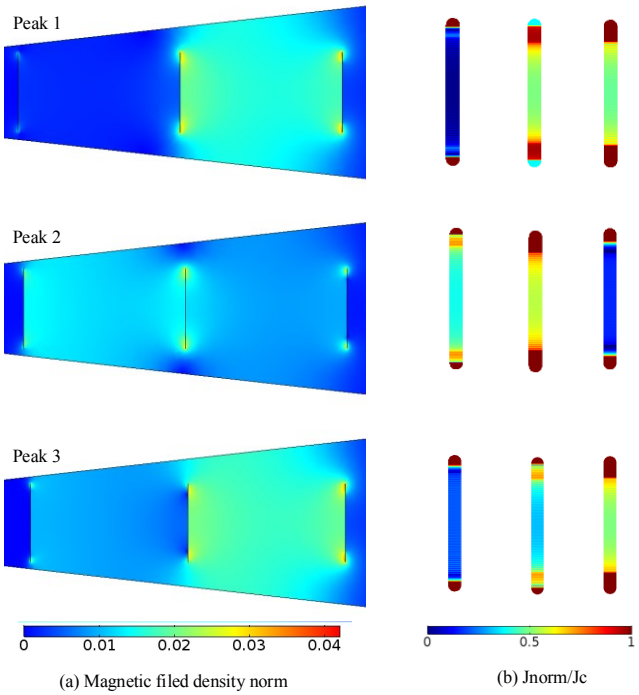

Fig. 9. Transport AC losses under balanced rated load with a harmonic current (10A, 200Hz)

IV. Conclusion

A FEM model of a HTS tri-axial CORC cable was constructed based on T-A formulation to study the influence of harmonic current on the AC losses of the cable used in hybrid electric aircraft. Firstly, when the cable operates without harmonic current, the simulation result shows a considerably imbalanced transport AC loss distribution even under balanced rated load. Losses produced in the outer phase can be two times larger than that in the inner phase. Then, after the harmonic currents are induced in three phases, even a small proportion (less than 10% of the rated current) of the harmonic currents can significantly increase the transport AC losses (up to 40%) of the tri-axial cable under rated load. Due

to the impact of the harmonic current on cable's AC losses, the amplitude and frequency of the harmonic current should be limited at a lowest possible level. Conclusion can also be made that the imbalanced electromagnetic coupling among three phases leads to a significantly non-uniform distribution of transport AC loss. An unbalanced load design will be required to balance the AC loss distribution among phases in the near future.

REFERENCES

[1] P. J. Masson and C. A. Luongo, "High power density superconducting motor for all-electric aircraft propulsion," *IEEE Transactions on Applied Superconductivity,* vol. 15, no. 2, pp. 2226-2229, 2005.

[2] P. J. Masson *et al.*, "Superconducting Ducted Fan Design for Reduced Emissions Aeropropulsion," *Ieee Transactions on Applied Superconductivity,* vol. 19, no. 3, pp. 1662-1668, Jun 2009.

[3] P. J. Masson, K. Ratelle, P. A. Delobel, A. Lipardi, and C. Lorin, "Development of a 3D Sizing Model for All-Superconducting Machines for Turbo-Electric Aircraft Propulsion," *Ieee Transactions on Applied Superconductivity,* vol. 23, no. 3, Jun 2013, Art. no. 3600805.

[4] P. J. Masson, D. S. Soban, E. Upton, J. E. Pienkos, and C. A. Luongo, "HTS motors in aircraft propulsion: Design considerations," *Ieee Transactions on Applied Superconductivity,* vol. 15, no. 2, pp. 2218-2221, Jun 2005.

[5] F. Berg, J. Palmer, P. Miller, M. Husband, and G. Dodds, "HTS Electrical System for a Distributed Propulsion Aircraft," *Ieee Transactions on Applied Superconductivity,* vol. 25, no. 3, Jun 2015, Art. no. 5202705.

[6] M. Zhang, F. Eastham, and W. J. Yuan, "Design and Modeling of 2G HTS Armature Winding for Electric Aircraft Propulsion Applications," *Ieee Transactions on Applied Superconductivity,* vol. 26, no. 3, Apr 2016, Art. no. 5205705.

[7] F. Berg, J. Palmer, P. Miller, and G. Dodds, "HTS System and Component Targets for a Distributed Aircraft Propulsion System," *Ieee Transactions on Applied Superconductivity,* vol. 27, no. 4, Jun 2017, Art. no. 3600307.

[8] L. Bertola, T. Cox, P. Wheeler, S. Garvey, and H. Morvan, "Superconducting Electromagnetic Launch System for Civil Aircraft," *Ieee Transactions on Applied Superconductivity,* vol. 26, no. 8, Dec 2016, Art. no. 3602911.

[9] J. D. Weiss, T. Mulder, H. J. ten Kate, and D. C. van der Laan, "Introduction of CORC (R) wires: highly flexible, round high-temperature superconducting wires for magnet and power transmission applications," *Superconductor Science & Technology,* vol. 30, no. 1, Jan 2017, Art. no. 014002.

[10] C. Barth, D. C. van der Laan, N. Bagrets, C. M. Bayer, K. P. Weiss, and C. Lange, "Temperature- and field-dependent characterization of a conductor on round core cable," *Superconductor Science & Technology,* vol. 28, no. 6, Jun 2015, Art. no. 065007.

[11] W. H. Fietz, M. J. Wolf, A. Preuss, R. Heller, and K. P. Weiss, "High-Current HTS Cables: Status and Actual Development," *Ieee Transactions on Applied Superconductivity,* vol. 26, no. 4, Jun 2016, Art. no. 4800705.

[12] P. C. Michael, L. Bromberg, D. C. van der Laan, P. Noyes, and H. W. Weijers, "Behavior of a high-temperature superconducting conductor on a round core cable at current ramp rates as high as 67.8 kAs(-1) in background fields of up to 19T," *Superconductor Science & Technology,* vol. 29, no. 4, Apr 2016, Art. no. 045003.

[13] M. A. Young *et al.*, "An investigation of the current distribution in the triaxial cable and its operational impacts on a power system," *IEEE Transactions on Applied Superconductivity,* vol. 15, no. 2, pp. 1751-1754, 2005.

[14] S. Fukui, T. Noguchi, J. Ogawa, M. Yamaguchi, T. Sato, and O. Tsukamoto, "Analysis of AC Loss and Current Distribution Characteristics of Multi-Layer Triaxial HTS Cable for 3-Phase AC Power Transmission," *IEEE Transactions on Applied Superconductivity,* vol. 16, no. 2, pp. 135-138, 2006.

[15] S. Fukui *et al.*, "Numerical Study on AC Loss Minimization of Multi-Layer Tri-Axial HTS Cable for 3-Phase AC Power Transmission," *IEEE Transactions on Applied Superconductivity,* vol. 17, no. 2, pp. 1700-1703, 2007.

[16] D. Miyagi, S. Iwata, N. Takahashi, and S. Torii, "3D FEM Analysis of Effect of Current Distribution on AC Loss in Shield Layers of Multi-Layered HTS Power Cable," *IEEE Transactions on Applied Superconductivity,* vol. 17, no. 2, pp. 1696-1699, 2007.

[17] T. Mulder *et al.*, "Design and Manufacturing of a 45 kA at 10 T REBCO-CORC Cable-in-Conduit Conductor for Large-Scale Magnets," *Ieee Transactions on Applied Superconductivity,* vol. 26, no. 4, Jun 2016, Art. no. 4803605.

[18] T. Mulder, A. Dudarev, M. Mentink, D. van der Laan, M. Dhalle, and H. ten Kate, "Performance Test of an 8 kA @ 10-T 4.2-K ReBCO-CORC Cable," *Ieee Transactions on Applied Superconductivity,* vol. 26, no. 4, Jun 2016, Art. no. 4803705.

[19] D. C. van der Laan *et al.*, "Engineering current density in excess of 200Amm(-2) at 20T in CORC (R) magnet cables containing RE-Ba2Cu3O7-delta tapes with 38 mu m thick substrates," *Superconductor Science & Technology,* vol. 28, no. 12, Dec 2015, Art. no. 124001.

[20] D. C. van der Laan *et al.*, "Record current density of 344Amm(-2) at 4.2K and 17T in CORC (R) accelerator magnet cables," *Superconductor Science & Technology,* vol. 29, no. 5, May 2016, Art. no. 055009.

[21] M. Majoros, M. D. Sumption, E. W. Collings, and D. C. van der Laan, "Magnetization losses in superconducting YBCO conductor-on-round-core (CORC) cables," *Superconductor Science & Technology,* vol. 27, no. 12, Dec 2014, Art. no. 125008.

[22] R. Terzioglu, M. Vojenciak, J. Sheng, F. Gomory, T. F. Ccedil;avus, and I. Belenli, "AC loss characteristics of CORC((R))cable with a Cu former," *Superconductor Science & Technology,* vol. 30, no. 8, Aug 2017, Art. no. 085012.

[23] M. Vojenciak *et al.*, "Magnetization ac loss reduction in HTS CORC (R) cables made of striated coated conductors," *Superconductor Science & Technology,* vol. 28, no. 10, Oct 2015, Art. no. 104006.

[24] E. Lavopa, P. Zanchetta, M. Sumner, and F. Cupertino, "Real-Time Estimation of Fundamental Frequency and Harmonics for Active Shunt Power Filters in Aircraft Electrical Systems," *IEEE Transactions on Industrial Electronics,* vol. 56, no. 8, pp. 2875-2884, 2009.

[25] H. Zhang, M. Zhang, and W. Yuan, "An efficient 3D finite element method model based on the T − A formulation for superconducting coated conductors," *Superconductor Science and Technology,* vol. 30, no. 2, p. 024005, 2016.

[26] F. Liang *et al.*, "A finite element model for simulating second generation high temperature superconducting coils/stacks with large number of turns," *Journal of Applied Physics,* vol. 122, no. 4, p. 043903, 2017.

[27] K. Kajikawa, T. Hayashi, R. Yoshida, M. Iwakuma, and K. Funaki, "Numerical evaluation of AC losses in HTS wires with 2D FEM formulated by self magnetic field," *Ieee Transactions on Applied Superconductivity,* vol. 13, no. 2, pp. 3630-3633, Jun 2003.

[28] V. M. R. Zermeno, A. B. Abrahamsen, N. Mijatovic, B. B. Jensen, and M. P. Sorensen, "Calculation of alternating current losses in stacks and coils made of second generation high temperature superconducting tapes for large scale applications," *Journal of Applied Physics,* vol. 114, no. 17, Nov 7 2013, Art. no. 173901.

[29] L. Queval, V. M. R. Zermeno, and F. Grilli, "Numerical models for ac loss calculation in large-scale applications of HTS coated conductors," *Superconductor Science & Technology,* vol. 29, no. 2, Feb 2016, Art. no. 024007.